

Small Triangulations of 4-Manifolds and the 4-Manifold Census

Rhuaidi Burke¹, Benjamin Burton¹, Jonathan Spreer²

¹School of Mathematics and Physics, The University of Queensland,
Brisbane, 4072, Queensland, Australia.

²School of Mathematics and Statistics, The University of Sydney,
Sydney, 2006, New South Wales, Australia.

Contributing authors: rhuaidi.burke@uq.edu.au; bab@maths.uq.edu.au;
jonathan.spreer@sydney.edu.au;

Abstract

We present a framework to classify PL-types of large censuses of triangulated 4-manifolds, which we use to classify the PL-types of all triangulated 4-manifolds with up to six pentachora. This is successful except for triangulations homeomorphic to the 4-sphere, $\mathbb{C}P^2$, and the rational homology sphere $QS^4(\mathbf{2})$, where we find at most four, three, and two PL-types respectively. We conjecture that they are all standard. In addition, we look at the cases resisting classification and discuss the combinatorial structure of these triangulations—which we deem interesting in their own rights.

Keywords: computational low-dimensional topology, triangulations, census of triangulations, 4-manifolds, PL standard 4-sphere, Pachner graph, mathematical software, experiments in low-dimensional topology

MSC Classification: 57-04 , 57-08 , 57-11 , 57Q15 , 57Q05 , 57Q25 , 57K40 , 57Q70 , 55U10 , 57R05 , 57K41

1 Introduction

In the context of computational topology it is desirable to have a data set of examples on which to perform experiments and test hypotheses. As such, an exhaustive list of all 4-manifold triangulations of a certain size and type, called a *census*, serves as such a useful reference. In dimension three we currently have censuses available with up

to 11 tetrahedra (containing 13 400 closed, orientable, prime, minimal triangulations). In dimension 4, where a closed 4-manifold requires an even number of pentachora, censuses are currently limited to triangulations with 2, 4, and 6 pentachora. However, despite this relative scarcity of data, even with just three tiers of the census, there are a total of 441 287 triangulations to consider.

Given a smooth manifold X , another smooth manifold X' is called *exotic (with respect to X)*, if X' is homeomorphic but not diffeomorphic to X . In other words, X and X' represent the same topological manifold but are distinct as smooth manifolds. Dimension four is the first dimension in which exotic smooth structures appear. It is a fundamental problem in 4-manifold topology to determine the number of smooth structures a particular 4-manifold admits. The simplest and most famous instance of this problem is the *Smooth 4-Dimensional Poincaré Conjecture* (S4PC for short):

Conjecture 1 (S4PC) There do not exist exotic 4-spheres.

It is typical to discuss exotic structures in relation to a ‘standard’ or canonical smooth structure. For example, the standard structure on \mathbb{R}^n is the one given by a single chart with the identity map; on \mathbb{S}^n it is the one with two charts given by stereographic projection.

Remark 1 The concept of a standard smooth structure is not well-defined in isolation. For instance, let $K3$ be the *K3 surface* with the standard smooth structure coming from being the zero-set of $w^4 + x^4 + y^4 + z^4 = 0$ in $\mathbb{C}P^3$, and let $\mathbb{C}P^2$ be the standard complex projective plane. Then each of the connected sums¹ $X_1 = \#_3 \mathbb{C}P^2 \#_{20} \overline{\mathbb{C}P^2}$ and $X_2 = K3 \# \overline{\mathbb{C}P^2}$ inherits a standard smooth structure from their summands. It is known that $X_1 \cong_{\text{TOP}} X_2$ but $X_1 \not\cong_{\text{DIFF}} X_2$ [1], meaning X_1 is exotic with respect to X_2 and vice versa. The smallest triangulations of two 4-manifolds that are known to be homeomorphic, but not diffeomorphic, are *ideal triangulations* (i.e. triangulations of manifolds with non-empty boundary where the boundary is given by a neighbourhood of a vertex) with 10 pentachora [2]. The authors are not aware of any triangulations of closed 4-manifolds which are homeomorphic, but not diffeomorphic, and which are not simply formed from a connected sum of ‘standard’ well-known manifolds (such as X_1 and X_2 above).

Cairns [3, 4] and Whitehead [5] show that every smooth n -manifold can be triangulated, that is, admits a piecewise-linear (PL) structure. Moreover, every PL n -manifold for $n \leq 6$ admits a compatible smooth structure which is unique up to diffeomorphism [6, 7]. Hence, there is a bijective correspondence between isotopy classes of smooth and PL structures on 4-manifolds, and so we speak of smooth and PL structures on a 4-manifold interchangeably.

¹Given two d -manifolds X and Y , their *connected sum*, written $X \# Y$ is formed by removing an open d -ball from each of X and Y and gluing them together along their resulting boundaries. We use $\#_k X$ to denote the k -fold connected sum of X with copies of itself. The operation is independent of the d -ball removed from their summands.

Related Work.

The past decade has seen significant interest in the problem of enumerating and classifying triangulations, including several other attempts at classifying and simplifying triangulations of 4-manifolds, particularly 4-spheres. Most recently, Pérez-Cerezo [8], building on the work of Joswig et al. [9], analysed the same census we investigate in this paper.

More broadly, there has been a growing body of utilising Pachner moves to either simplify triangulations or establish PL-homeomorphisms. For example, the work Björner and Lutz [10], Lutz and Tsuruga [11], the second author [12], Altmann and the third author [13], the second and third author [14], and more recently the first author [2]. We note that whilst Björner, Lutz, Joswig et al., and Tsuruga, and (to some extent) Pérez-Cerezo use *simplicial complexes*, the work of the authors and Altmann instead use *generalised triangulations* (see Section 2.1). These are more ‘flexible’ than simplicial complexes since, for example we allow two facets of the same simplex to be identified.

Contributions.

We study the census of triangulations of closed, orientable, 4-manifolds with up to 6 pentachora. This data set contains 8 triangulations with 2 pentachora, 784 triangulations with 4 pentachora, and 440 495 triangulations with 6 pentachora. It includes a variety of triangulations with interesting combinatorial and topological features (see Tables 1 to 3 for a breakdown of numbers of triangulations by (PL-)topological types). The dataset was first generated by Budney and the second author [15] using *tricensus*, a utility of [16].

In addition, we present a new algorithm for finding PL-homeomorphisms between large numbers of 4-manifold triangulations by combining original heuristics and computational tools. This algorithm yields a near complete classification of the PL-types in the census. We note that, due to the undecidability of the 4-manifold homeomorphism problem [17], we can only hope for heuristics which for as many cases as possible, give the correct answer, in as short a time as possible. We also investigate the combinatorial structure of the triangulations resisting classification.

Specifically, we improve on the results of Pérez-Cerezo, reducing the upper bounds on the number of potential PL classes for $\mathbb{C}P^2$ and \mathbb{S}^4 : within the set of 6-pentachoron triangulations homeomorphic to $\mathbb{C}P^2$, we reduce the number of potential PL classes from 5 down to 3; within the set of 4-pentachoron triangulations homeomorphic to \mathbb{S}^4 , we reduce from 3 to 2; and finally for the set of 6-pentachoron triangulations homeomorphic to \mathbb{S}^4 , we obtain at most 4 potential classes, down from 36 in [8].

Acknowledgements.

The authors would like to thank Ryan Budney for his contributions at an early stage of this project. The authors would also like to thank the anonymous referees for insightful comments that improved the presentation of this paper. This paper was finished whilst the first author was visiting the University of Sydney, and thanks the University of Sydney for their hospitality. The third author is supported by the Australian Research Council’s Discovery funding scheme (project no. DP190102259).

2 Preliminaries

In Section 2.1 and Section 2.2 we review some of the basic theory of (generalised) triangulations and local moves on triangulations. In Section 2.3 and Section 2.4 we recap some of the classical results in 4-manifold theory and handle decompositions.

2.1 Triangulations

We refer to a 4-simplex as a *pentachoron* (plural: *pentachora*). The tetrahedral cells of a pentachoron are referred to as *facets*. We label the vertices of a pentachoron by elements of $\{0, 1, 2, 3, 4\}$, and use the convention that facet i refers to the facet opposite to the vertex labelled by i . A (*generalised, 4-dimensional*) *triangulation* \mathcal{T} is a finite collection of n abstract pentachora, some or all of whose $5n$ facets are affinely identified (‘glued’) in pairs. More precisely, let $\tilde{\Delta} = \{\Delta_0, \Delta_1, \dots, \Delta_{n-1}\}$ be a set of n pentachora, and let $\Phi = \{\varphi_0, \dots, \varphi_{m-1}\}$ be a set of at most $m \leq 2n$ *face gluings*, such that each φ_i is an affine identification between two distinct facets of simplices, and each facet is a part of at most one such identification. We write $\Delta_i(a)$ to denote vertex a of pentachoron Δ_i , and $\Delta_i(abcd)$ to denote the facet $abcd$ of Δ_i (and analogous notation for edges and triangles). A face gluing $\varphi \in \Phi$ is then explicitly described by an expression of the form $\Delta_i(abcd) \leftrightarrow \Delta_j(efgh)$, which means that facet $abcd$ of Δ_i is mapped to facet $efgh$ of Δ_j such that $a \leftrightarrow e$, $b \leftrightarrow f$, $c \leftrightarrow g$, and $d \leftrightarrow h$. Our triangulation is defined to be $\mathcal{T} := \tilde{\Delta}/\Phi$ the identification space obtained under the natural quotient map $q : \tilde{\Delta} \rightarrow \mathcal{T}$. In other words, the data specifying a triangulation are the triple $(\tilde{\Delta}, \Phi, q)$. The (*real*) *boundary* of \mathcal{T} consists of all the facets that are not identified with any other facets. Figure 1a depicts a typical triangulation.

Remark 2 Such triangulations are also referred to as an *unordered Δ -complex*.

Remark 3 These triangulations are typically far more efficient than simplicial complexes since, for example, we allow two facets of the same pentachoron to become identified.

Remark 4 Our triangulations as defined above are not *a priori* triangulations “of something” (for example a manifold); they are, initially at least, purely abstract combinatorial objects. One must check certain conditions hold to conclude that the triangulation has the structure of a manifold (for example, that the link—defined below—of each vertex is homeomorphic to either \mathbb{S}^3 or B^3).

The gluings defining \mathcal{T} also have the effect of merging vertices, edges, triangles, and tetrahedra of the pentachora into equivalence classes, which we refer to as the *vertices*, *edges*, *triangles*, and *tetrahedra* of \mathcal{T} .

The *link* $\text{lk}(v)$ of a vertex v of \mathcal{T} , is the ‘frontier’ of a small regular neighbourhood of v . We treat vertex links as triangulated 3-dimensional spaces, formed by inserting a small tetrahedron into each corner of each pentachoron, and then joining together the tetrahedra from adjacent pentachora along their triangular faces. This mirrors

the traditional concept of a link in a simplicial complex, but is modified to support generalised triangulations.

If v lies in the boundary of \mathcal{T} , its link is a space with boundary. If the link is homeomorphic to B^3 , then we refer to v as a *boundary vertex*. If the link is any other space with boundary then we say v is an *invalid vertex*. On the other hand, if v does not lie in the boundary of \mathcal{T} , its link is a closed space. If the link is (PL-)homeomorphic to S^3 , then v is an *internal vertex*, and if it is any other closed space then it is referred to as an *ideal vertex*.

We insist that no edge of \mathcal{T} is identified with itself in reverse, and that no triangle is identified with itself via a non-identity permutation. This, together with the condition that the link of every vertex is either B^3 or S^3 , guarantees that \mathcal{T} triangulates a 4-manifold.

Given a triangulation \mathcal{T} of a 4-manifold, the vector $f(\mathcal{T}) = (f_0, f_1, f_2, f_3, f_4)$, where f_i denotes the number of i -dimensional faces in \mathcal{T} , is called its *face vector*, or *f-vector* for short. Since \mathcal{T} triangulates a 4-manifold, it satisfies the following equations

$$-2f_3 + 5f_4 = 0 \tag{1}$$

$$2f_1 - 3f_2 + 4f_3 - 5f_4 = 0 \tag{2}$$

$$f_0 - f_1 + f_2 - f_3 + f_4 = \chi(\mathcal{T}) \tag{3}$$

known as *generalised Dehn–Sommerville equations* [18]. Here, $\chi(\mathcal{T})$ denotes the *Euler characteristic* of \mathcal{T} , a topological invariant. Observe that Equation (1) implies that a triangulation of a closed 4-manifold must have an even number of pentachora.

To encode a triangulation, we give each pentachoron a label and an ordering of its five vertices. Two triangulations are (*combinatorially isomorphic*) if they are identical up to relabelling of pentachora and/or reordering of the pentachoron vertices. We can uniquely identify any isomorphism class of triangulations using an efficiently-computable string called an *isomorphism signature* [12]. Every triangulation has a unique isomorphism signature, and two triangulations have the same signature if and only if they are isomorphic.

An important tool in the study of triangulations is the *dual graph* (also known as the *face pairing graph*). Given a triangulation \mathcal{T} , its dual graph $\Gamma(\mathcal{T}) = (V, E)$ is the multigraph whose nodes are the pentachora in \mathcal{T} , and for each gluing that identifies two tetrahedral facets of p_i and p_j we add an arc between the corresponding nodes in V . By construction, $\Gamma(\mathcal{T})$ has maximum degree ≤ 5 , and is 5-regular when \mathcal{T} triangulates a closed 4-manifold $\Gamma(\mathcal{T})$. Figure 1b depicts a typical dual graph.

The dual graph as defined above does not retain any information about the permutations used in the face identifications, and so \mathcal{T} cannot be reconstructed from $\Gamma(\mathcal{T})$ alone. Nevertheless, some information about the underlying topology of the 4-manifold can still be extracted from $\Gamma(\mathcal{T})$. It also proves to be useful as a visual tool when discussing triangulations.

Housekeeping 1. In order to avoid confusion, we use the terms *vertices* and *edges* exclusively when referring to triangulations, and *nodes* and *arcs* when referring to graphs.

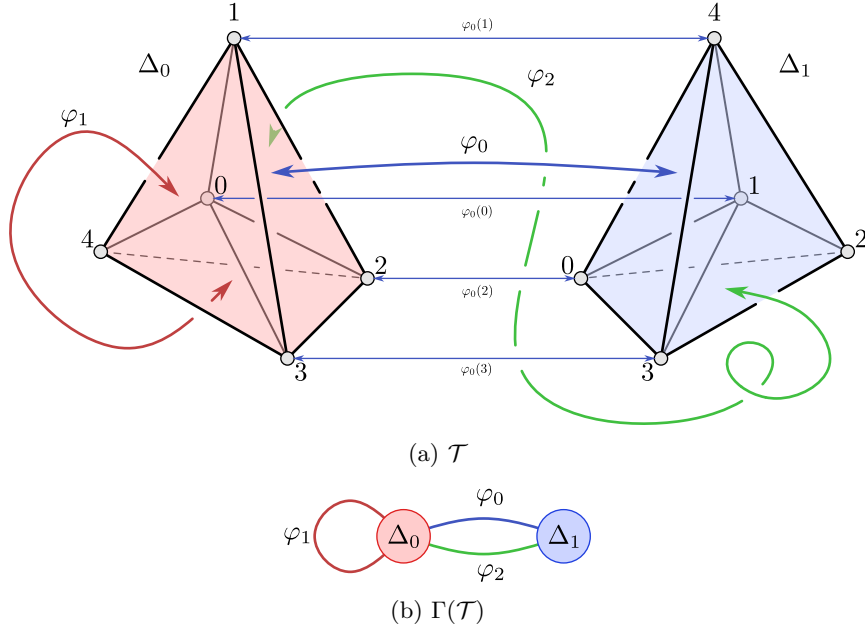


Fig. 1: (a) A triangulation $\mathcal{T} = \tilde{\Delta}/\Phi$ with two pentachora $\tilde{\Delta} = \{\Delta_0, \Delta_1\}$ and three face gluings $\Phi = \{\varphi_0, \varphi_1, \varphi_2\}$. The map φ_0 is given by $\Delta_0(0123) \xrightarrow{\varphi_0} \Delta_1(1403)$. (b) The dual graph $\Gamma(\mathcal{T})$ of the triangulation \mathcal{T} .

2.2 Local Moves and the Pachner Graph

We modify our triangulations using *Pachner moves* (or *bistellar flips*), which are local moves that change a triangulation but not its underlying PL-type [19]. Informally, an (i, j) Pachner move can be thought of as taking a subcomplex of i pentachora in the boundary complex of the 5-simplex $\partial\Delta^5$, and replacing them with its complement in $\partial\Delta^5$ of $6 - i = j$ pentachora. This necessarily means that (a) the i pentachora share a common $(5 - i)$ -dimensional face – which is removed from the triangulation; and (b) the j pentachora share a common $(i - 1)$ -face – which is newly inserted into the triangulation. See Figure 2 for an illustration of Pachner moves in dimension four, and see [19] for more details.

The use of Pachner moves has several key benefits: Firstly, two PL manifolds X , and X' are PL-homeomorphic if and only if there exists a sequence of Pachner moves between X and X' . This statement is known as *Pachner's theorem* and was first proven in [19]. We can therefore certify that two triangulations are PL-homeomorphic by finding a connecting sequence of Pachner moves. Even without a guarantee that this algorithm will terminate, it is effective in practice. Secondly, Pachner moves can be used to reduce the size of a triangulation (without changing the underlying PL-type). Finally, Pachner moves are already implemented and ready-to-use in several software packages. Here, we use *Regina* [16].

The *Pachner graph* of a PL manifold X , denoted by $\mathcal{P}(X)$, is used to describe and track how distinct triangulations of a 4-manifold can be related via Pachner moves. It is the (infinite) graph with nodes corresponding to isomorphism classes of triangulations of X ; and two nodes of $\mathcal{P}(X)$ are joined by an arc if and only if there is a single Pachner move that takes one triangulation to the other. We refer the reader to [12] for further details.

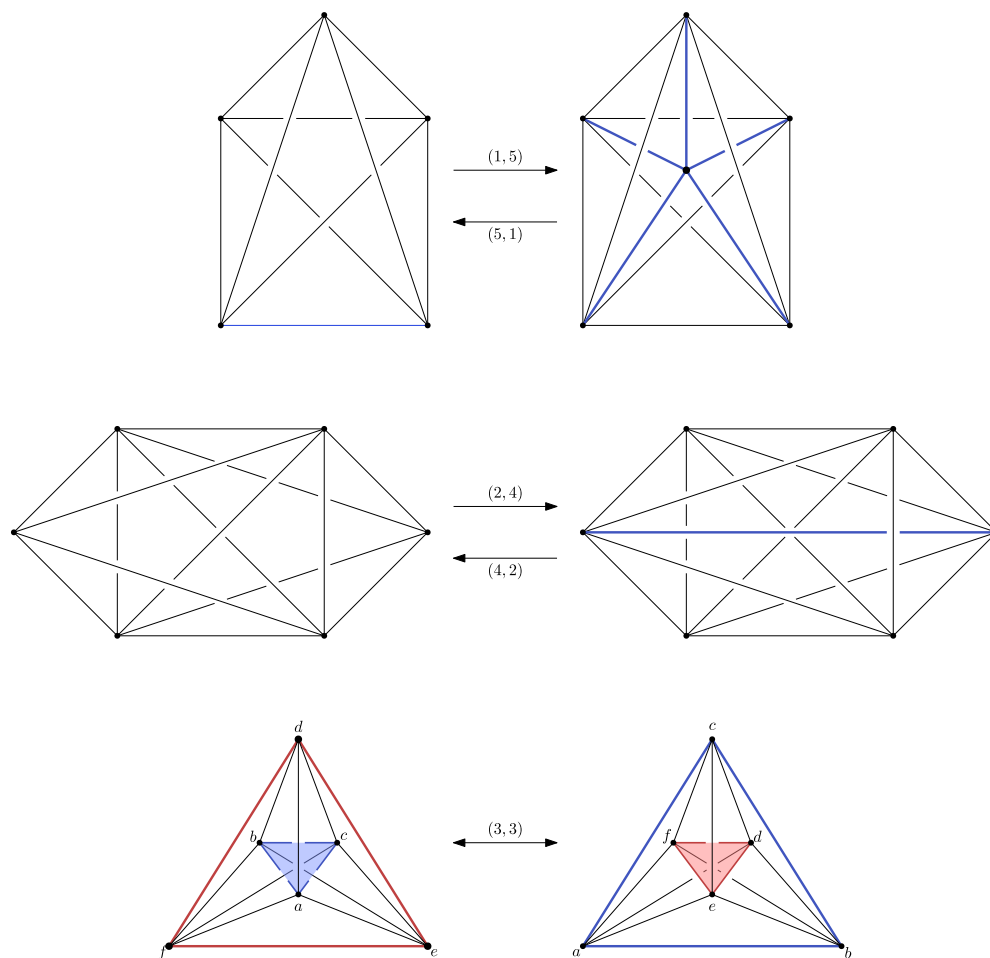


Fig. 2: Pachner moves and their inverses in dimension 4

There are many other local modifications which can be expressed by sequences of Pachner moves. When moving through the Pachner graph, using these additional modifications can be powerful, since they allow the use of ‘short-cuts’ into different areas of the graph. In this article, we make extensive use of two of these additional moves, the *2-0-Edge move* and the *2-0-Triangle move*. The *2-0-Edge move* takes two

pentachora, identified along three tetrahedra to form a ‘pillow’ around a common edge, and flattens them to form two tetrahedra. The 2-0-Triangle move is similar. Here, two pentachora, are identified along two tetrahedra to form a pillow around a common triangle, and flattens them to form three tetrahedra.

2.3 4-Manifolds

Let \mathcal{T} be a 4-manifold triangulation. For the *ring of coefficients* \mathbb{Z} , the *group of p -chains*, $0 \leq p \leq 4$, denoted $C_p(\mathcal{T}, \mathbb{Z})$, of \mathcal{T} is the group of formal sums of p -dimensional faces with \mathbb{Z} coefficients. The *boundary operator* is a linear operator $\partial_p : C_p(\mathcal{T}, \mathbb{Z}) \rightarrow C_{p-1}(\mathcal{T}, \mathbb{Z})$ defined by

$$\partial_p \sigma = \partial_p \{v_0, \dots, v_p\} = \sum_{j=0}^p \{v_0, \dots, \widehat{v}_j, \dots, v_p\},$$

where σ is a face of \mathcal{T} , $\{v_0, \dots, v_p\}$ represents σ as a face of a pentachoron of \mathcal{T} in local vertices v_0, \dots, v_p , and \widehat{v}_j means v_j is deleted from the list.

Denote by $Z_p(\mathcal{T}, \mathbb{Z})$ and $B_{p-1}(\mathcal{T}, \mathbb{Z})$ the kernel and the image of ∂_p respectively. Observing $\partial_p \circ \partial_{p+1} = 0$, we define the *p -th homology group* $H_p(\mathcal{T}, \mathbb{Z})$ of \mathcal{T} by the quotient $H_p(\mathcal{T}, \mathbb{Z}) = Z_p(\mathcal{T}, \mathbb{Z})/B_p(\mathcal{T}, \mathbb{Z})$. Each homology group H_p is a finitely generated \mathbb{Z} -module, and is a topological invariant of the manifold triangulated by \mathcal{T} . We write $\beta_p = \dim(H_p(\mathcal{T}, \mathbb{Z}))$ for the dimension of (the free part of) H_p . Informally, $H_p(\mathcal{T}, \mathbb{Z})$, $0 \leq p \leq 4$, of a triangulation \mathcal{T} counts the number of ‘ p -dimensional holes’ in \mathcal{T} . For a more thorough introduction to homology theory see [20].

Let X be a closed, oriented 4-manifold. Representatives of classes in $H_2(X; \mathbb{Z})$ generically intersect in a finite number of points (possibly after isotoping them into transverse position). The *intersection form* Q_X of X , is the symmetric, unimodular, bilinear form defined by

$$Q_X : H_2(X; \mathbb{Z}) \times H_2(X; \mathbb{Z}) \rightarrow \mathbb{Z}, \quad Q_X(\alpha, \beta) = S_\alpha \cdot S_\beta := \sum_{S_\alpha \cap S_\beta} \pm 1,$$

where S_α , and S_β are 2-chains representing the classes $\alpha, \beta \in H_2(X; \mathbb{Z})$. If X is smooth, S_α , and S_β can be chosen to be oriented surfaces embedded in X [21, Proposition 1.2.3].

A landmark result of 4-manifold topology is the following classification result for simply connected (i.e. having trivial fundamental group²) topological 4-manifolds due to Freedman.

Theorem 1 (Freedman [22]) *For every symmetric, unimodular, bilinear form Q , there exists a closed simply connected topological 4-manifold X such that $Q_X = Q$. If Q is even, this manifold is unique up to homeomorphism. If Q is odd then there are exactly two different homeomorphism types of manifolds with the given intersection form, however only at most one of these admits a PL structure.*

²The *fundamental group* of a manifold X , denoted $\pi_1(X)$, describes closed paths in X up to homotopy, with the group operation of path concatenation.

Shortly after Freedman's result, Donaldson showed the following equally important result.

Theorem 2 (Donaldson [23]) *The symmetric unimodular bilinear form $\oplus_m[+1]$ is the only positive definite form that can be realised as the intersection form of a PL 4-manifold.*

The results by Freedman and Donaldson (together with Serre's algebraic classification of indefinite forms) imply the following key result.

Theorem 3 *Two simply connected PL 4-manifolds are homeomorphic if and only if their intersection forms have the same rank, signature, and parity.*

Housekeeping 2. All manifolds are assumed to be PL/smooth, closed, connected, and orientable, unless explicitly stated otherwise.

Example 1 The 4-sphere \mathbb{S}^4 has no 2-homology and so $Q_{\mathbb{S}^4} = \emptyset$. The complex projective plane, $\mathbb{C}P^2$, has $Q_{\mathbb{C}P^2} = [+1]$, and the oppositely oriented manifold $\overline{\mathbb{C}P^2}$ has $Q_{\overline{\mathbb{C}P^2}} = [-1]$. $S^2 \times S^2$ has intersection form $Q_{S^2 \times S^2} = \begin{bmatrix} 0 & 1 \\ 1 & 0 \end{bmatrix}$.

2.4 Handle Decompositions and Kirby Diagrams

In the smooth setting, we primarily work with 4-manifolds via *handle decompositions*. Let X, X' be two smooth 4-manifolds. We say X is obtained from X' by attaching a (4-dimensional) k -handle, denoted $X = X' \cup_{\varphi} h^k$, if there is an embedding

$$\varphi : S^{k-1} \times D^{4-k} \rightarrow \partial X'$$

such that X is of the form

$$X = [X' \sqcup D^k \times D^{4-k}] / \varphi(x) \sim x,$$

where D^k denotes the closed k -disk ($k \in \{1, 2, 3, 4\}$). There always exists a Morse function $f : X \rightarrow \mathbb{R}$ inducing a handle decomposition $X = \bigcup_{i=0}^n X_i$ with

$$\emptyset = X_{-1} \subset X_0 \subset \cdots \subset X_n = X$$

in which X_i is obtained from X_{i-1} by attaching i -handles [24]. Since X is closed and connected, it can be assumed that there is a single 0- and 4-handle. Hence a closed 4-manifold X is obtained from B^4 by attaching 1-, 2-, and 3-handles and finally capping off with another B^4 . Given such a handle decomposition, we depict X by drawing the attaching regions of the handles in the boundary of the 0-handle ($\partial B^4 \cong \mathbb{S}^3 \cong \mathbb{R}^3 \cup \{*\}$). By a result of Laudenbach and Poenaru [25], 3- and 4-handles attach

uniquely up to diffeomorphism, and so it suffices to understand how the 1- and 2-handles attach. We depict 1-handles by ‘dotted’ unknots (see Section 5.4 of [21] for details of this notation). A 2-handle is attached via a map of the form $S^1 \times D^2 \rightarrow S^3$. These maps are determined up to isotopy by (i) an embedding $S^1 \times \{0\} \rightarrow S^3$ (i.e. a *knot*) and (ii) a choice of normal vector field on the knot. Classes of such vector fields are in non-canonical bijection with the integers [21]. Once a choice for $0 \in \mathbb{Z}$ has been made—the so-called *0-framing* f_0 —any other framing differs from f_0 by some integral number of twists. By convention, we make the choice that the normal vector field induced from the collar of any Seifert surface S of K is the zero framing. Fixing an orientation of K gives a well-defined notion of linking number, and if we consider a parallel push-off K' of K along the surface S then $\text{lk}(K, K') = 0$. This is referred to as the *canonical framing* (or *Seifert framing*).

As such, we draw a 2-handle as a knot decorated with an integer. A decorated link diagram of this form—dotted unknots and integer decorated links, together with a specification of how many 3- and 4-handles there are—is called a *Kirby diagram* and gives a combinatorial encoding of a closed 4-manifold up to diffeomorphism. Figure 3 is an example of a typical Kirby diagram.

3 Topological Classification

In this section we describe a classification of the triangulations in the census up to topological homeomorphism. This serves as a spring board to then carry out the PL classification. We start by grouping the triangulations of the census by their homology groups. Since all manifolds under consideration are closed and orientable, we omit $H_0(X; \mathbb{Z}) \cong H_4(X; \mathbb{Z}) \cong \mathbb{Z}$ from the homology vector, i.e. we simply refer to $(H_1(X; \mathbb{Z}), H_2(X; \mathbb{Z}), H_3(X; \mathbb{Z}))$. In a second step, and in the case of simply connected triangulations, we use *Regina*’s built-in intersection form routine and Theorem 3 to split these groups further.

For the remaining triangulations, we simply guess their topological types, build triangulations of these manifolds (using *Katie*, see Section 4.4, and built-in functionality of *Regina*), and compare them to the census manifolds using Pachner moves (that is, we establish a PL homeomorphism). Altogether, this leads to the following classification, summarised in Tables 1, 2, and 3 (note that the content of the fourth column refers to work done in Section 4). In Table 2, we begin to see the appearance of S^1 -bundles over *lens spaces*, denoted $L(p, q)$, which are important class of 3-manifold obtained by gluing two solid tori together (see [26] for more).

Table 1: Topological classification of the closed orientable 2-pentachoron census.

# Pentachora	4-Manifold	# Triangulations	# PL Classes
2	\mathbb{S}^4	6	1
	$S^3 \times S^1$	2	1

Table 2: Topological classification of the closed orientable 4-pentachoron census.

# Pentachora	4-Manifold	# Triangulations	# PL Classes
4	\mathbb{S}^4	647	≤ 2
	$S^3 \times S^1$	126	1
	$\mathbb{C}P^2$	4	1
	$S^3 \times S^1 \# \mathbb{C}P^2$	3	1
	$\mathbb{R}P^3 \times S^1$	1	1
	$L(3, 1) \times S^1$	1	1
	$L(3, 1) \tilde{\times} S^1$	2	1

Rational Homology 4-Spheres with Finite Fundamental Group

Before giving the table for six pentachora, we first define a particular family of 4-manifolds. Let $R(n)$ denote the 4-manifold given by the Kirby diagram in Figure 3, in which there are n strands wrapping around the 1-handle.

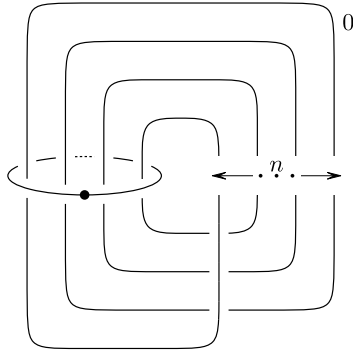


Fig. 3: A Kirby diagram of the rational ball $R(n)$

This 4-manifold $R(n)$ is a *rational homology ball*—that is, it has the same homology as a 4-sphere when one computes the homology with rational coefficients. Let $QS^4(n)$ denote the double of $R(n)$, that is

$$QS^4(n) := DR(n) = R(n) \cup_{\text{id}} R(n).$$

The 4-manifold $QS^4(n)$ is then a *rational homology 4-sphere* with $\pi_1(QS^4(n)) \cong \mathbb{Z}_n$ and homology vector $(\mathbb{Z}_n, \mathbb{Z}_n, 0)$. By using a combination of *Katie*, UP-SIDE-DOWN-SIMPLIFY (see Section 4), and *Regina*, we obtain representative triangulations of $QS^4(n)$ for $n \in \{2, 3\}$, each with six pentachora respectively.

Remark 5 We note that the topological type of $QS^4(n)$ was not identified in [8].

Table 3: Topological classification of the closed orientable 6-pentachoron census.

# Pentachora	4-Manifold	# Triangulations	# PL Classes
6	\mathbb{S}^4	405 188	≤ 4
	$S^3 \times S^1$	29 124	1
	$\mathbb{C}P^2$	4 423	≤ 3
	$S^2 \times S^2$	5	1
	$S^2 \tilde{\times} S^2$	7	1
	$\#_2 \mathbb{C}P^2$	8	1
	$S^3 \times S^1 \# \mathbb{C}P^2$	1 477	1
	$S^3 \times S^1 \#_2 \mathbb{C}P^2$	6	1
	$\mathbb{R}P^3 \times S^1$	42	1
	$L(3, 1) \times S^1$	55	1
	$L(3, 1) \tilde{\times} S^1$	64	1
	$L(4, 1) \times S^1$	3	1
	$L(4, 1) \tilde{\times} S^1$	3	1
	$L(5, 2) \times S^1$	1	1
	$L(5, 2) \tilde{\times} S^1$	1	1
	$QS^4(2)$	84	≤ 2
	$QS^4(3)$	4	1

4 The PL classification algorithm

In this section we present our search heuristic to establish piecewise linear homeomorphisms between large quantities of triangulated manifolds conjectured to be in the same PL class. We first start by going over some subroutines before sketching the algorithm as a whole.

4.1 Important subroutines

UP-SIDE-DOWN-SIMPLIFY (USDS): This subroutine is the heart of our algorithm. It is relatively easy to describe, but details are very important. We point out that it is difficult to design a method which is efficient for both triangulations that can trivially be merged with a different class, as well as pathological cases needing millions, if not billions of moves to escape a local area of the Pachner graph (apart from the triangulation presented in Section 5 resisting classification altogether, there are four more 4-pentachoron triangulations requiring a large number of moves before being classified as standard). Extensive research has been done to find effective strategies to compare PL homeomorphism types for triangulated 4-manifolds, see Section 1 for a detailed discussion. At least in the case of the census of small 4-manifold triangulations, the below strategy yields the best results on a consistent basis.

Our heuristic is a slight variation of a standard biased Markov chain-style random walk through the Pachner graph of a triangulation. We bias the sizes of the triangulations visited by the random walk around a fixed target size of \hat{n} pentachora (in our calculations, we used $8 \leq \hat{n} \leq 12$). If the current state of the random walk has more than \hat{n} pentachora, an exponential penalty is imposed on choosing a Pachner move

further increasing the size of the state. The same is true for a current state of smaller size than \hat{n} and moves further reducing its size.

The core idea of our approach lies in the type of moves we choose to increase and decrease the sizes of our triangulations: we use 2-4-Pachner moves to increase the size of a triangulation, but 2-0- edge- and triangle-moves to reduce the size of a triangulation. Moreover, we use standard 3-3-Pachner moves to change triangulations while keeping their f -vector constant.

Empirical evidence suggest, that this approach mixes triangulations much faster than by just using standard Pachner moves. This approach has already been used very successfully by the first author [2] in the search of minimal triangulations. The method used there is even simpler in structure than the one presented below.

Our base method has four input parameters that stay fixed for the duration the method is run: (a) A set probability $x \in [0, 1]$ to decide whether a 3-3-move or some other move is performed, (b) a target size \hat{n} for triangulations to be visited in the random walk, (c) a parameter $\alpha \in \mathbb{R}$ determining the severity of the penalty for sampling a triangulation of size away from \hat{n} , and (d) a number of steps $s \in \mathbb{Z}$.

Heuristic 1

Setup:

- $x \in [0, 1], \alpha \in \mathbb{R}, \hat{n} \in \mathbb{Z}, s \in \mathbb{Z}$

Main Loop:

- Set $\mathcal{T} = \mathcal{T}_0$
- For each step $1 \leq i \leq s$ and while $|\mathcal{T}| \neq n$:
 1. Update $\mathcal{T} = \mathcal{T}'$
 2. Update $\beta = \frac{e^{\alpha(\hat{n}-|\mathcal{T}|)}}{1+e^{\alpha(\hat{n}-|\mathcal{T}|)}} \in [0, 1]$
 3. Sample $u \in \mathcal{U}([0, 1])$
 4. Case $u > x$: if available, do 3-3-move on \mathcal{T} to return triangulation \mathcal{T}'
 5. Sample $v \in \mathcal{U}([0, 1])$
 6. If $v > \beta$: if available, perform 2-0-Edge- or Triangle-move on \mathcal{T} to return triangulation \mathcal{T}'
 7. Perform 2-4-move on \mathcal{T} to return triangulation \mathcal{T}'
- If \mathcal{T} and \mathcal{T}_0 are in different classes, merge classes

ADJUST-VERTEX-NUMBER: This subroutine takes a triangulated 4-manifold \mathcal{T}_0 as input, and outputs a PL homeomorphic triangulation with v vertices.

If \mathcal{T}_0 has fewer than v vertices, perform 1-5-moves $v - f_0(\mathcal{T}_0)$ times to obtain a v -vertex triangulation. If, on the other hand, the input triangulation has more than v vertices, we randomly perform edge collapses. If not enough edge collapses are available, we run USDS in between until they become available. It is worthwhile noting that the latter case has no guarantee to terminate in general, but does very quickly in practice.

4.2 The Algorithm

Our implementation is based on establishing PL-homeomorphisms using Pachner’s theorem [19], i.e. by describing sequences of Pachner moves transforming one triangulation into another. Our computations are organised in a UNION-FIND structure: at any step of our calculations, every triangulation is associated to a class of triangulations for which pairwise PL homeomorphisms have already been established. Each class has a unique representative triangulation. If a sequence of Pachner moves is found turning a triangulation from one class into a triangulation from another class, both classes are merged with the representative of the latter class, and we continue. This way, if the task is to classify N triangulations, we only need to establish $O(N)$, rather than $O(N^2)$ PL homeomorphisms.

We start with a large number of triangulations $\mathcal{T}_1, \dots, \mathcal{T}_N$. Here, we assume that all triangulations have the same number of n pentachora, but this is not necessary for the algorithm to work. We furthermore assume that we have already established that all triangulations \mathcal{T}_i , $1 \leq i \leq N$, are homeomorphic. Again, this is not a necessary requirement for the algorithm to work, but we require, however, that all triangulations have already been tested to have the same Euler characteristic m .

For n -pentachora triangulations of Euler characteristic m , it is a consequence of Section 2.1 that their f -vector is determined by their number of vertices. We have the following algorithm.

Main Algorithm

1. Initialise UNION-FIND structure with N classes $\{\mathcal{T}_i\}$, $1 \leq i \leq N$, of size 1.
2. Fix $v = \min\{f_0(\mathcal{T}_i) | 1 \leq i \leq N\}$, the smallest number of vertices found in our list.
3. For all $1 \leq i \leq N$:
 - (a) Use ADJUST-VERTEX-NUMBER to produce a v -vertex triangulation \mathcal{T}'
 - (b) Use USDS to connect \mathcal{T}' to \mathcal{T}_j , $f_0(\mathcal{T}_j) = v$, $f_4(\mathcal{T}_j) = n$, from the list
Once this step is complete, every PL class has a v -vertex representative.
4. For all classes, run USDS to connect its representative to a new class. Use a moderate time-out threshold to skip hard cases.
5. As long as there are still more than K classes, goto **6**.
6. For remaining classes, run USDS with relaxed parameters.

4.3 Implementation, Timings, and Remarks

Our implementation of the algorithm described in this section is available at <https://github.com/raburke/Dim4Census/>.

Our guiding principle for the implementation is to minimise human intervention. We point out that we can modify arbitrarily many triangulations in parallel until they can be merged with an existing class of the UNION-FIND structure. This parallelises the bottleneck of the computation for large censuses of largely easy-to-handle triangulations. When dealing with pathologically difficult combinatorial structures, running

different random walks on the same triangulation may lead to similar speed-ups. However, for the 6-pentachoron census with its $\approx 400,000$ triangulations, parallelisation is not crucial and we hence defer its implementation to future work.

For some indications of running times, we ran our algorithm on a laptop with an 11th Gen Intel i7 processor and 32GB of RAM, with input the 405 188 6-pentachoron triangulations homeomorphic to S^4 . We obtained the following timings, summarised in Table 4, for first running ADJUST-VERTEX-NUMBER (referred to as *Step 1*), then running USDS until only 10 classes are left over (*Step 2*), and then the times to merge any additional class until we reduce to 6 classes, which is when we stopped our calculations.

Table 4: Sample running times of the Main Algorithm with input 405 188 6-pentachoron 4-spheres.

Step 1 (s)	Step 2 (s)	9 cl (s)	8 cl (s)	7 cl (s)	6 cl (s)	Total time (s)
13 686	10 752	88	4 787	11 008	4 987	45 308
14 061	10 306	373	1 097	335	1 143	27 315
14 170	9 264	365	451	464	3 754	28 468
14 182	9 359	1 116	1 772	99	3 772	30 300
14 142	9 791	405	811	1 598	7 961	34 708
13 212	9 342	302	48	3 100	3 155	29 159

Achieving 5 connected classes usually does not take much longer (with 1 611 and 18 929 additional seconds in two of the six runs summarised above). Achieving four class takes around a week, as we were able to observe on multiple occasions. The algorithm never achieved 3 classes. Running the complete algorithm in parallel on 100+ cores may produce additional results. Alternatively, exhaustive enumeration on a larger machine with more memory may lead to additional merges of classes.

PL classification of other topological types was achieved through a combination of exhaustive enumeration and our main algorithm. Relevant timings are summarised in Table 5.

Table 5: Sample running times of PL classification for selected manifolds.

Manifold	Step 1 (s)	Step 2 (s)	1 cl (s)	Total time (s)
$S^3 \times S^1$	2480	119	51	2650
$S^2 \times S^2$	115	0	4 514	4 629
$\#_2 \mathbb{C}P^2$	27	0	1 531	1 558
$S^3 \times S^1 \# \mathbb{C}P^2$	1 060	140	42	1 242
$S^3 \times S^1 \#_2 \mathbb{C}P^2$	0	0	62 022	62 022

4.4 *Katie* and PL Classification Results

As discussed in Section 4, our PL classification algorithm determines whether two given triangulations are PL homeomorphic. What is missing from this algorithm is a reference triangulation for which its PL homeomorphism type is known.

For this we use the software tool *Katie* [2, 27], developed by the first author. *Katie* is based on an algorithm due to Casali and Cristofori [28]. It takes as input a Kirby diagram and produces a triangulation of the associated PL 4-manifold. For each of the topological types in Tables 1 to 3, we start with the Kirby diagram representing its canonical PL-type, and compare the resulting triangulation to the triangulations in the census.

For all but three topological types, all triangulations homeomorphic to a given 4-manifold, are pairwise PL-homeomorphic. The three exceptions are \mathbb{S}^4 , $\mathbb{C}P^2$, and the \mathbb{Q} -homology sphere $QS^4(2)$, cf. Table 3 for which we find 4, 3, and 2 classes respectively.

As already documented in Section 4.3, our algorithm reliably takes all 405 188 triangulations homeomorphic to \mathbb{S}^4 from the 6-pentachoron census and classifies them into around 5 PL classes within a day of computation time. Some of the remaining classes have remarkable combinatorial properties, which are discussed in more detail in Section 5. These remaining classes are certified to be impossible to connect to other classes using an exhaustive enumeration and traversal of the Pachner graph with an excess height of 6 (that is, only triangulations with number of pentachora up to $6 + 6 = 12$ are considered).

In some contrast to the triangulations homeomorphic to \mathbb{S}^4 , we can connect all but four of the 29 124 triangulations homeomorphic to $S^3 \times S^1$ using exhaustive simplification and traversal of the Pachner graph, with an excess height of at most four. The remaining four can be confirmed to be standard $S^3 \times S^1$ s by (i) retriangulating to show they were all PL-homeomorphic to each other, and then (ii) traversing the Pachner graph with an excess height of at most 6. Alternatively, using our algorithm, all 29 124 triangulations homeomorphic to $S^3 \times S^1$ can be connected within an hour of computation time, see Section 4.3.

This difference in behaviour is noteworthy since \mathbb{S}^4 and $S^3 \times S^1$ are the only two closed orientable 4-manifolds which can be triangulated using only 2 pentachora.

5 Pathological Triangulations, Combinatorial Obstructions, and 2-Knots

In this section we will present some preliminary analysis of, and discuss ideas concerning, the triangulations still resisting classification. We focus our attention for now on the unique 4-pentachoron 4-sphere which we were unable to connect to the standard 4-sphere. The sphere in question, which we will denote by Q , has isomorphism signature `eAMPcaabcddd+aoa+aAa8aQara`. The dual graph of Q is depicted in Figure 4. The colouring of the graph will be explained as required throughout the section.

The 2-pentachoron subcomplex consisting of pentachora 2 and 3 of Q also appears within many of the other triangulations resisting classification (for example, the

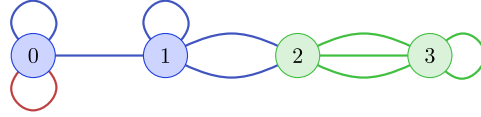


Fig. 4: The dual graph of Q

6-pentachoron CP^2 s). The subcomplex in question, denoted C , has isomorphism signature cHIbbb0bRbpb , f -vector $f = (1, 1, 5, 6, 2)$, and boundary an ideal 2-tetrahedron solid torus.

Considered in isolation C is not a triangulation of a manifold: its single vertex link is a pinched genus-4 handlebody, and the link of its single edge is a thrice-punctured sphere. However, the boundary of C can be uniquely closed up to produce an ideal triangulation of a 4-manifold. Performing the gluing $\Delta_0(0234) \leftrightarrow \Delta_0(0312)$ yields the unique³ 2-pentachoron ideal triangulation of a *Cappell–Shaneson 2-knot* complement, first analysed by Budney–Burton–Hillman [29], and which we will denote by CS . This is an ideal triangulation of the complement of a *knotted 2-sphere* Σ in the 4-sphere, $S^4 - \nu\Sigma$ (where $\nu\Sigma$ denotes a tubular neighbourhood of Σ). By knotted, we mean that Σ does not bound an embedded 3-ball in S^4 . The Cappell–Shaneson 2-knot triangulation considered in [29] is just one in a family of knotted 2-spheres in S^4 , which are in a sense parametrised by elements of $GL(\mathbb{Z}^3)$ and their traces [30]. The 2-knot of [29] corresponds to one such $A \in GL(\mathbb{Z}^3)$ with trace 0.

In addition to the study of 2-knots being an interesting pursuit in its own right, 2-knots have also appeared as an important source of examples for constructing potential counterexamples to S4PC via the *Gluck construction*, which goes as follows. Given a knotted 2-sphere Σ in S^4 , remove a tubular neighbourhood of Σ (i.e. a copy of $\Sigma \times D^2$) and reglue it by the self-diffeomorphism of $S^2 \times S^1$ which rotates the S^2 factor once as one travels around S^1 . The result is a topological 4-sphere but which in general is not known to be diffeomorphic to the standard 4-sphere. However, it has been shown that for many classes of 2-knots, the result is indeed a standard S^4 : for example, twist-spun knots (discussed further in Section 6.2) [31, 32], doubles of ribbon disks (Exercise 6.2.11(b) [21]), and various Cappell–Shaneson 2-knots [33–36].

The ‘cut-open’ Cappell–Shaneson complex C embeds in a topological 4-ball B_C^4 , which is itself obtained by ungluing a single facet identification of Q (depicted by the red arc in Figure 4). The isomorphism signature of B_C^4 is $\text{eGzMkabcdddcaGa8aAa0awa}$. Perhaps the first point of interest with regards to B_C^4 is that even the presentation of its fundamental group is challenging to simplify, with a presentation given by

$$\langle a, b \mid a^3 b^3 a^{-2} b^{-2}, a^{-3} b^{-1} a^5 b^2 \rangle.$$

Using GAP, we are able to verify that the order of the group is 1, and hence is indeed the trivial group. We note that GAP uses coset enumeration to compute the order in this case, rather than performing any kind of simplification heuristic, for example via a sequence of Tietze transformations.

³Verifiable via a very short exhaustive search of the ideal 2-pentachoron census.

Moreover, it is worthwhile to note that when B_C^4 is attached to a larger triangulation, the B_C^4 subcomplex remains intact through very large flip sequences. For example, attaching B_C^4 to a minimal triangulation of $S^2 \times S^2 - D^4$ produces a new triangulation of a topological $S^2 \times S^2$ which we are unable to (re)simplify to the original triangulation of $S^2 \times S^2$. Similarly for many other choices of 4-manifold.

In this sense, C , or B_C^4 , is a potential combinatorial obstruction to simplifying triangulations it appears within (similar to the topological ‘dunce hat’ being a combinatorial obstruction to collapsing a contractible space). The fact that all five triangles of C are in fact dunce hats perhaps gives some, albeit naive, evidence in support of this idea. In other words, one might wonder if C constitutes a kind of higher-dimensional analogue of the dunce hat.

Whilst the 4-sphere Q does not appear to be directly obtained from the Cappell–Shaneson 2-knot itself via the Gluck construction—since truncating the ideal vertex of CS and attaching a $S^2 \times D^2$ to the resulting real boundary yields triangulations of the 4-sphere which we are able to successfully simplify to a minimal triangulation of the standard 4-sphere—it nevertheless still seems tempting to assume that Q relates in some way to the Cappell–Shaneson 4-spheres, in light of the complex C and its relation to CS .

We have the following results and conjectures concerning B_C^4 and Q .

Conjecture 2 The topological 4-ball B_C^4 is PL-homeomorphic to the standard 4-ball.

We conjecture that B_C^4 supports the standard PL structure because of its small size and previously discussed connection to Cappell–Shaneson sphere which is known to be standard.

Proposition 4 *If there exists a sequence of Pachner moves connecting Q to a triangulation of the standard PL 4-sphere, then this sequence must contain at least one triangulation with at least 12 pentachora.*

Proof Running an exhaustive enumeration of all local move sequences starting from Q and visiting triangulations up to 10 pentachora (i.e. an excess height of 6) does not connect Q to any other 4-pentachoron triangulation of the 4-sphere. \square

6 Ongoing and Future Work

To conclude this article, we detail how to extend the observations made in the previous section and, more broadly, in this article, to two research directions for future work.

6.1 The 8-Pentachoron Census

Generating a census (of any type) with n simplices consists of two stages: First, enumerate all possible dual graphs with n nodes; then, for each graph, test all possible $5n/2$ facet gluings and retain those that yield valid triangulations. For 2, 4, and 6

pentachora there are 3, 26, and 638 such graphs, leading to 8, 784, and 440 495 valid 4-manifold triangulations, respectively.

We can deduce from this that only a very small fraction of possible gluings give rise to a triangulation of a 4-manifold, implying that various optimisations are possible (and needed) to build the census even only up to 6 pentachora (cf. [37–39] for an overview of such optimisations in the 3-dimensional setting). In the case of 8 pentachora however, existing optimisations appear to no longer be sufficient. Consequently, entirely new algorithms are in development to complete this next step of the 4-dimensional census. A completed 8-pentachoron census will come with new challenges for classifying their PL-types. Undoubtedly, more interesting pathological triangulations will emerge and in greater numbers. This is work in progress.

6.2 More 2-Knot Complements – Generation and Classification

The Cappell–Shaneson 2-knot complement discussed at the beginning of this section is only one of many such topological objects that can be described using only a small number of pentachora. In theory, each of them can lead to difficult triangulations of 4-balls and 4-spheres, related to B_C^4 and S_C^4 . Such examples are very useful for constructions in low-dimensional topology, or to benchmark future iterations of search methods. Given such a collection of examples, the major challenge is to either rigorously quantify how difficult they are to simplify, or to relate them to former or present potential counterexamples to S4PC.

It would therefore seem worthwhile to attempt to enumerate (and ideally, also classify) triangulations of 2-knot complements. This would provide us with a wealth of examples with which to construct interesting 4-sphere triangulations.

Whilst we currently do not have a means of constructing triangulations of arbitrary 2-knot complements, we do have several sources of examples and construction techniques for certain classes of 2-knots. One of the first techniques for constructing non-trivial 2-knots was the *spinning construction* due to Artin [40], which can be described as follows. Let $K : S^1 \rightarrow \mathbb{R}^3$ be a classical 1-knot. One can always isotope K such that it lies in the upper half space $\mathbb{R}_+^3 = \{(x, y, z) : z \geq 0\}$ except for an unknotted arc which lies below the xy -plane. Remove the interior of this unknotted arc to obtain a knotted arc in \mathbb{R}_+^3 with its endpoints in the x - y plane. Now rotate \mathbb{R}_+^3 about \mathbb{R}^2 through \mathbb{R}^4 via the map which sends a point $(x, y, z) \in \mathbb{R}_+^3$ to $(x, y, z \cos \theta, z \sin \theta) \in \mathbb{R}^4$ ($0 \leq \theta < 2\pi$). In this way, the knotted arc sweeps out a knotted S^2 in \mathbb{R}^4 (moreover the 2-knot obtained through this method is independent of the arc removed from the original 1-knot).

The latest release of *Regina* (version 7.4) now includes functionality to produce a triangulation of the complement of such a *spun knot*, given a 1-knot as input. This provides us with as many triangulations of 2-knot complements as there are 1-knots.

A generalisation of the spinning construction, due to Zeeman [41], involves also rotating the knotted arc itself independently by a whole number of twists whilst the ‘sweep-out’ through \mathbb{R}^4 takes place; this gives the so-called *k-twist spun* of the knot K , denoted $\tau_k(K)$. As of the time of writing, we have only implemented an algorithm to construct ‘regular’ (i.e. 0-twist) spun knots in *Regina*, and so it is a point of future work to extend this construction to the *k-twist* case.

The second source of examples is the ideal census with up to 6-pentachora which has also already been generated (though not yet classified in its entirety). It is not difficult to identify potential candidates for 2-knot complements within the census: a triangulation of a 2-knot complement has the same homology as \mathbb{S}^1 , and has boundary $S^2 \times S^1$. If we wish to further filter out potential ‘unknots’ (i.e. triangulations of $S^1 \times B^3$) then we filter out triangulations with fundamental group isomorphic to \mathbb{Z} and look for more interesting fundamental groups. From such a list of candidates, in order to conclude that a given triangulation is indeed the complement of an embedded S^2 in a 4-sphere, one needs to verify that attaching a $S^2 \times D^2$ to the boundary of a given candidate produces a 4-sphere.

Using this process, we were able to (i) completely classify the ideal census with 2 pentachora (Table 6); (ii) find complements of non-trivial 2-knots with 4 pentachora; and (iii) find candidates for complements of non-trivial 2-knots with 6 pentachora. Note that in the 2-pentachoron census presented in Table 6, since the triangulations are of manifolds with ideal boundary, the manifolds labelled $L(p, q) \times I$ can also be understood as double cones over $L(p, q)$. All triangulations within a given row were determined to be PL-homeomorphic and hence we do not list the number of PL classes.

Table 6: Classification of the ideal orientable 2-pentachoron census.

4-Manifold	# Triangulations
$S^1 \times B^3$	3
Cappell–Shaneson Trace 0	1
$L(3, 1) \times I$	1
$L(4, 1) \times I$	1
$L(5, 2) \times I$	1

Of the 3366 triangulations within the ideal 4-pentachoron census, we identified 1754 triangulations of $S^1 \times B^3$ and 54 non-trivial 2-knot complements. Note that in general, unlike 1-knots, 2-knots are not determined by their complement (nor fundamental group) [30]; hence names in Table 7 should be treated as an ‘alias’ for convenience (and indeed for the final two rows of Table 7 this reference label is largely meaningless as we have yet to determine a known label for these 2-knots; the subscripts refer vaguely to the fundamental group).

Issa [42] has produced triangulations of Cappell–Shaneson complements up to trace 20 (along with the associated 4-spheres), which enabled us, by direct comparison, to identify the particular Cappell–Shaneson knots within the census. Similarly, again by direct construction and comparison, we were able to identify the 2-twist spins of the trefoil and figure-eight knots, denoted by $\tau_2(3_1)$ and $\tau_2(4_1)$ respectively, in the table. Since *Regina* does not currently support k -twist spun knots for $k > 0$, the method of construction we employed was by exploiting the fact that the 2-twist spin of a 2-bridge knot $K(p, q)$ is fibred by the punctured lens space, which we denote by $L(p, q)^\circ$ [41, 43].

By first constructing $L(p, q)^\circ$ and then using *Regina's* `bundleWithMonodromy` function we obtained triangulations with the correct topology. After simplifying, we were then able to demonstrate PL-homeomorphisms with those triangulations which appeared in the census. It is known that fibred 2-knots with fibre a punctured lens space are in fact determined by their complement [44].

We make the following conjectures regarding the identities of the complements labelled by K_{3*3} and $K_{3,3}$. Firstly, we conjecture that K_{3*3} is the complement of a 2-cable of the 2-twist spun trefoil (see [43] for the definition of cabling in the context of 2-knots). Second, $K_{3,3}$ is the complement of a 1-roll spun Figure-8 [45]. Evidence for both of these claims come from an analysis of their fundamental groups. In the case of K_{3*3} , its fundamental group is

$$\pi_1 \cong \mathbb{Z} \rtimes_{\varphi} (\mathbb{Z}_3 * \mathbb{Z}_3),$$

where $\varphi(1) = \psi \in \text{Aut}(\mathbb{Z}_3 * \mathbb{Z}_3)$ with $\psi(a) = b$ and $\psi(b) = a^{-1}$. This aligns with what we would expect to see from a 2-cable of the 2-twist spun of the trefoil—a fibred 2-knot with fibre $(L(3, 1) \# L(3, 1))^\circ$.

For $K_{3,3}$, one of the triangulations has fundamental group with presentation

$$\langle a, b \mid aba^{-1}bab^{-1} = 1, a^3b^3 = 1 \rangle,$$

which can be rewritten as

$$\langle a, b \mid aba = bab, a^3 = b^3 \rangle,$$

which was shown to be the fundamental group of the 1-roll spun Figure-8 [45]. It may be possible to verify these claims constructively in the same manner as with the 2-twist spun examples, however the limited construction algorithms currently available make this strategy difficult to realise. Developing algorithms allowing us to triangulate arbitrary n -twist m -roll spun knots is a point for further research.

The triangulations are available to study via a *Regina* data file in the GitHub repository (<https://github.com/raburke/Dim4Census/>).

Table 7: Table of 4-pentachoron 2-knot complements

Label	# Triangulations
$S^1 \times B^3$	1 754
Cappell–Shaneson Trace 0	38
Cappell–Shaneson Trace 1	2
Cappell–Shaneson Trace 2	1
$\tau_2(3_1)$	3
$\tau_2(4_1)$	1
K_{3*3}	1
$K_{3,3}$	8

A preliminary search also revealed that out of the 405 188 6-pentachoron triangulations of the 4-sphere, 256 of them contained a 4-pentachoron subcomplex corresponding to a ‘cut open’ 2-knot complement (in the same vein as in the case of C and Q). A point of future work is to determine how difficult these particular spheres are to simplify.

In terms of the 6-pentachoron census, as of the time of writing we have only carried out a very coarse preliminary filtering and classification. The ideal 6-pentachoron census contains some 2 787 568 triangulations. Of these we identified 1 088 164 triangulations homeomorphic to $S^1 \times B^3$ and 8 467 candidates for non-trivial 2-knot complements. Using the new `spun` function in *Regina* we were able to identify 7 PL-homeomorphic triangulations of the (0-twist) spun trefoil, $\tau_0(3_1)$. Similarly, we found zero triangulations PL-homeomorphic to $\tau_0(4_1)$ (and our current best efforts to obtain a small triangulation of $\tau_0(4_1)$ yields a triangulation with 16 ideal pentachora). In light of these last two points and the observations from the 4-pentachoron ideal census—namely the triangulations of $\tau_2(3_1)$ and $\tau_2(4_1)$ —we conclude with the following question.

Question 1. Does the complement of $\tau_2(K(p, q))$ always require fewer pentachora to triangulate than $\tau_0(K(p, q))$?

We hope for the preliminary results and ideas discussed in this section to be the subject of future work dedicated specifically to triangulations of 2-knot complements and related constructions.

References

- [1] Kronheimer, P.B., Mrowka, T.S.: Recurrence relations and asymptotics for four-manifold invariants. *Bull. Amer. Math. Soc. (N.S.)* **30**(2), 215–221 (1994) <https://doi.org/10.1090/S0273-0979-1994-00492-6>
- [2] Burke, R.A.: Practical software for triangulating and simplifying 4-manifolds. *Journal of Computational Geometry* **16**(2), 109–144 (2025) <https://doi.org/10.20382/jocg.v16i2a4>
- [3] Cairns, S.S.: Triangulation of the manifold of class one. *Bull. Amer. Math. Soc.* **41**(8), 549–552 (1935) <https://doi.org/10.1090/S0002-9904-1935-06140-3>
- [4] Cairns, S.S.: A simple triangulation method for smooth manifolds. *Bull. Amer. Math. Soc.* **67**, 389–390 (1961) <https://doi.org/10.1090/S0002-9904-1961-10631-9>
- [5] Whitehead, J.H.C.: On C^1 -complexes. *Ann. of Math. (2)* **41**, 809–824 (1940) <https://doi.org/10.2307/1968861>
- [6] Hirsch, M.W., Mazur, B.: *Smoothings of Piecewise Linear Manifolds*. *Annals of Mathematics Studies*, vol. No. 80, p. 134. Princeton University Press, Princeton, NJ (1974)

- [7] Munkres, J.: Obstructions to the smoothing of piecewise-differentiable homeomorphisms. *Ann. of Math. (2)* **72**, 521–554 (1960) <https://doi.org/10.2307/1970228>
- [8] Pérez-Cerezo, F.A.: Inspection of a Census of 4-Manifolds. Master’s Thesis (2024)
- [9] Joswig, M., Lofano, D., Lutz, F.H., Tsuruga, M.: Frontiers of sphere recognition in practice. *J. Appl. Comput. Topol.* **6**(4), 503–527 (2022) <https://doi.org/10.1007/s41468-022-00092-8>
- [10] Björner, A., Lutz, F.H.: Simplicial manifolds, bistellar flips and a 16-vertex triangulation of the Poincaré homology 3-sphere. *Experiment. Math.* **9**(2), 275–289 (2000)
- [11] Tsuruga, M., Lutz, F.H.: Constructing Complicated Spheres (2013). <https://arxiv.org/abs/1302.6856>
- [12] Burton, B.A.: The Pachner graph and the simplification of 3-sphere triangulations. In: *Proc. 27th ACM Symp. Comput. Geom. (SoCG 2011)*, Paris, France, June 13–15, 2011, pp. 153–162. ACM, New York (2011). <https://doi.org/10.1145/1998196.1998220>
- [13] Altmann, E.G., Spreer, J.: Sampling triangulations of manifolds using Monte Carlo methods. arXiv:2310.07372. Preprint, to appear in *Exp. Math.* Acceptance date: 8 Nov 2024 (2024)
- [14] Burton, B.A., Spreer, J.: Computationally proving triangulated 4-manifolds to be diffeomorphic (2014). <https://arxiv.org/abs/1403.2780>
- [15] Budney, R., Burton, B.A.: A census of small triangulated 4-manifolds. In preparation (2025)
- [16] Burton, B.A., Budney, R., Pettersson, W., et al.: Regina: Software for low-dimensional topology. Version 7.2 (1999–2022). <https://regina-normal.github.io>
- [17] Markov, A.A.: The insolubility of the problem of homeomorphy. *Dokl. Akad. Nauk SSSR* **121**, 218–220 (1958)
- [18] Sommerville, D.M.Y.: The relations connecting the angle-sums and volume of a polytope in space of n dimensions. *Proceedings of the Royal Society of London. Series A, Containing Papers of a Mathematical and Physical Character* **115**(770), 103–119 (1927). Accessed 2023-11-27

- [19] Pachner, U.: Konstruktionsmethoden und das kombinatorische Homöomorphieproblem für Triangulationen kompakter semilinearer Mannigfaltigkeiten. *Abh. Math. Sem. Univ. Hamburg* **57**, 69–86 (1987) <https://doi.org/10.1007/BF02941601>
- [20] Hatcher, A.: *Algebraic Topology*, p. 544. Cambridge University Press, Cambridge, Cambridge (2002)
- [21] Gompf, R.E., Stipsicz, A.I.: *4-Manifolds and Kirby Calculus*. Graduate Studies in Mathematics, vol. 20, p. 558. American Mathematical Society, Providence, RI (1999). <https://doi.org/10.1090/gsm/020>
- [22] Freedman, M.H.: The topology of four-dimensional manifolds. *J. Differential Geometry* **17**(3), 357–453 (1982)
- [23] Donaldson, S.K.: An application of gauge theory to four-dimensional topology. *J. Differential Geom.* **18**(2), 279–315 (1983)
- [24] Milnor, J., Spivak, M., Wells, R.: *Morse Theory*. (AM-51), Volume 51. Princeton University Press, Princeton, NJ (1969). <http://www.jstor.org/stable/j.ctv3f8rb6> Accessed 2024-12-01
- [25] Laudenbach, F., Poénaru, V.: A note on 4-dimensional handlebodies. *Bull. Soc. Math. France* **100**, 337–344 (1972)
- [26] Saveliev, N.: *Lectures on the Topology of 3-Manifolds: An Introduction to the Casson Invariant*, 2nd edn. De Gruyter Textbook, p. 207. Walter de Gruyter & Co., Berlin (2012). <https://doi.org/10.1515/9783110250367>
- [27] Burke, R.A.: *Katie*. Version 2.0 (2024). <https://github.com/raburke/Comp4Top>
- [28] Casali, M.R., Cristofori, P.: Kirby diagrams and 5-colored graphs representing compact 4-manifolds. *Rev. Mat. Complut.* **36**(3), 899–931 (2023) <https://doi.org/10.1007/s13163-022-00438-x>
- [29] Budney, R., Burton, B.A., Hillman, J.: Triangulating a Cappell-Shaneson knot complement. *Math. Res. Lett.* **19**(5), 1117–1126 (2012) <https://doi.org/10.4310/MRL.2012.v19.n5.a12>
- [30] Cappell, S.E., Shaneson, J.L.: There exist inequivalent knots with the same complement. *Ann. of Math. (2)* **103**(2), 349–353 (1976) <https://doi.org/10.2307/1970942>
- [31] Gordon, C.M.: Knots in the 4-sphere. *Comment. Math. Helv.* **51**(4), 585–596 (1976) <https://doi.org/10.1007/BF02568175>
- [32] Pao, P.S.: Nonlinear circle actions on the 4-sphere and twisting spun knots. *Topology* **17**(3), 291–296 (1978) [https://doi.org/10.1016/0040-9383\(78\)90033-2](https://doi.org/10.1016/0040-9383(78)90033-2)

- [33] Akbulut, S.: Cappell-Shaneson homotopy spheres are standard. *Ann. of Math.* (2) **171**(3), 2171–2175 (2010) <https://doi.org/10.4007/annals.2010.171.2171>
- [34] Gompf, R.E.: Killing the Akbulut-Kirby 4-sphere, with relevance to the Andrews-Curtis and Schoenflies problems. *Topology* **30**(1), 97–115 (1991) [https://doi.org/10.1016/0040-9383\(91\)90036-4](https://doi.org/10.1016/0040-9383(91)90036-4)
- [35] Gompf, R.E.: More Cappell-Shaneson spheres are standard. *Algebr. Geom. Topol.* **10**(3), 1665–1681 (2010) <https://doi.org/10.2140/agt.2010.10.1665>
- [36] Iwaki, K.: Infinite families of standard cappell-shaneson homotopy 4-spheres. *Topology and its Applications* **366**, 109293 (2025) <https://doi.org/10.1016/j.topol.2025.109293>
- [37] Burton, B.A.: Efficient enumeration of 3-manifold triangulations. *Austral. Math. Soc. Gaz.* **31**(2), 108–114 (2004)
- [38] Burton, B.A.: Enumeration of non-orientable 3-manifolds using face-pairing graphs and union-find. *Discrete Comput. Geom.* **38**(3), 527–571 (2007) <https://doi.org/10.1007/s00454-007-1307-x>
- [39] Burton, B.A., Pettersson, W.: An Edge-Based Framework for Enumerating 3-Manifold Triangulations. In: Arge, L., Pach, J. (eds.) 31st International Symposium on Computational Geometry (SoCG 2015). *Leibniz International Proceedings in Informatics (LIPIcs)*, vol. 34, pp. 270–284. Schloss Dagstuhl – Leibniz-Zentrum für Informatik, Dagstuhl, Germany (2015). <https://doi.org/10.4230/LIPIcs.SOCG.2015.270>
- [40] Artin, E.: Zur Isotopie zweidimensionaler Flächen im R_4 . *Abh. Math. Sem. Univ. Hamburg* **4**(1), 174–177 (1925) <https://doi.org/10.1007/BF02950724>
- [41] Zeeman, E.C.: Twisting spun knots. *Trans. Amer. Math. Soc.* **115**, 471–495 (1965) <https://doi.org/10.2307/1994281>
- [42] Issa, A.: Triangulating Cappell–Shaneson homotopy 4-spheres (2017). <https://core.ac.uk/download/162230035.pdf>
- [43] Teragaito, M.: Fibered 2-knots and lens spaces. *Osaka J. Math.* **26**(1), 57–63 (1989)
- [44] Plotnick, S.P., Suci, A.I.: Fibered knots and spherical space forms. *J. London Math. Soc.* (2) **35**(3), 514–526 (1987) <https://doi.org/10.1112/jlms/s2-35.3.514>
- [45] Fox, R.H.: Rolling. *Bull. Amer. Math. Soc.* **72**, 162–164 (1966) <https://doi.org/10.1090/S0002-9904-1966-11467-2>